

# Singlet-Oxygen-Induced Phospholipase A<sub>2</sub> Inhibition: A Major Role for Interfacial Tryptophan Dioxidation

Zahra Nasri,<sup>\*[a]</sup> Seyedali Memari,<sup>[a, b]</sup> Sebastian Wenske,<sup>[a]</sup> Ramona Clemen,<sup>[a]</sup> Ulrike Martens,<sup>[c, d]</sup> Mihaela Delcea,<sup>[c, d]</sup> Sander Bekeschus,<sup>[a]</sup> Klaus-Dieter Weltmann,<sup>[a]</sup> Thomas von Woedtke,<sup>[a, e]</sup> and Kristian Wende<sup>\*[a]</sup>

**Abstract:** Several studies have revealed that various diseases such as cancer have been associated with elevated phospholipase A<sub>2</sub> (PLA<sub>2</sub>) activity. Therefore, the regulation of PLA<sub>2</sub> catalytic activity is undoubtedly vital. In this study, effective inactivation of PLA<sub>2</sub> due to reactive species produced from cold physical plasma as a source to model oxidative stress is reported. We found singlet oxygen to be the most relevant active agent in PLA<sub>2</sub> inhibition. A more detailed analysis of the plasma-treated PLA<sub>2</sub> identified tryptophan 128 as a hot spot, rich in double oxidation. The

significant dioxidation of this interfacial tryptophan resulted in an N-formylkynurenine product via the oxidative opening of the tryptophan indole ring. Molecular dynamics simulation indicated that the efficient interactions between the tryptophan residue and phospholipids are eliminated following tryptophan dioxidation. As interfacial tryptophan residues are predominantly involved in the attaching of membrane enzymes to the bilayers, tryptophan dioxidation and indole ring opening leads to the loss of essential interactions for enzyme binding and, consequently, enzyme inactivation.

## Introduction

Phospholipase A<sub>2</sub> (PLA<sub>2</sub>) is a group of membrane proteins that specifically cleaves the acyl ester bond at the *sn*-2 position of glycerophospholipids, releasing fatty acids and

lysophospholipids.<sup>[1]</sup> The mammalian genome encodes more than 30 PLA<sub>2</sub> isoforms or related enzymes. The PLA<sub>2</sub> superfamily has three primary classification: secretory PLA<sub>2</sub> (sPLA<sub>2</sub>), cytosolic PLA<sub>2</sub> (cPLA<sub>2</sub>), and Ca<sup>2+</sup>-independent PLA<sub>2</sub> (iPLA<sub>2</sub>). The activity of PLA<sub>2</sub> isoforms leads to the release of a mixture of bioactive lipids or lipid mediators. Lysophosphatidic acid (LPA) is one such bioactive phospholipid produced by the enzymatic action of PLA<sub>2</sub>. It has been found to induce many cancer hallmarks, including cellular processes such as proliferation, growth, survival, migration, invasion, and angiogenesis promotion.<sup>[2]</sup> PLA<sub>2</sub> overexpression is not only associated with numerous cancers,<sup>[3]</sup> but also with inflammation in pathological processes such as asthma or allergy.<sup>[4]</sup> Moreover, increased PLA<sub>2</sub> activity has been reported in autoimmune disorders,<sup>[5]</sup> schizophrenia,<sup>[6]</sup> autism,<sup>[7]</sup> and bipolar disorders.<sup>[8]</sup> Therefore, elevated PLA<sub>2</sub> activity may play a role in the aforementioned disease states, and the regulation of its activity is of great interest. Several PLA<sub>2</sub> inhibitors have been developed so far: Nevertheless, there has been no reported clinical successes to date and no treatments have reached the market.<sup>[9]</sup> Hence, novel strategies for the effective and safe inhibition of PLA<sub>2</sub> are highly desirable.

Two regions are known to be involved in the PLA<sub>2</sub> activity; first, the interface site responsible for the enzyme binding to the membrane and the catalytic site.<sup>[10]</sup> Accordingly, the lack of efficient binding to the lipid membrane leads to a reduction of enzymatic activity. Interfacial bindings are formed primarily by hydrophobic amino acids, of which tryptophan plays a significant role.<sup>[11]</sup> Leslie et al. reported that the association of the catalytic domain of human cPLA<sub>2</sub> with the membrane is mediated in part by a tryptophan residue located at the membrane-exposed face of the enzyme.<sup>[12]</sup> Mutation of this tryptophan residue significantly reduced the membrane association of the enzyme.<sup>[13]</sup> It is also known that tryptophan plays

[a] Dr. Z. Nasri, S. Memari, S. Wenske, R. Clemen, Dr. S. Bekeschus, Prof. K.-D. Weltmann, Prof. T. von Woedtke, Dr. K. Wende  
Center for Innovation Competence (ZIK) *plasmatis*  
Leibniz Institute for Plasma Science and Technology (INP)  
Felix-Hausdorff-Straße 2, 17489, Greifswald, Germany  
E-mail: zahra.nasri@inp-greifswald.de  
kristian.wende@inp-greifswald.de

[b] S. Memari  
Institute of Anatomy and Cell Biology  
University Medicine Greifswald  
Friedrich-Loeffler-Straße 2, 17489, Greifswald, 17487, Germany

[c] Dr. U. Martens, Prof. M. Delcea  
Institute of Biochemistry  
University of Greifswald  
Felix-Hausdorff-Straße 4, Greifswald, 17489, Germany

[d] Dr. U. Martens, Prof. M. Delcea  
Center for Innovation Competence (ZIK) HIKE (Humoral Immune Reactions  
in Cardiovascular Diseases)  
University of Greifswald, Greifswald  
Fleischmannstraße 42, 17489, Germany

[e] Prof. T. von Woedtke  
Institute for Hygiene and Environmental Medicine  
University Medicine Greifswald, Greifswald  
Walther-Rathenau-Straße 49 A, 17489, Germany

 Supporting information for this article is available on the WWW under <https://doi.org/10.1002/chem.202102306>

 © 2021 The Authors. Chemistry - A European Journal published by Wiley-VCH GmbH. This is an open access article under the terms of the Creative Commons Attribution Non-Commercial License, which permits use, distribution and reproduction in any medium, provided the original work is properly cited and is not used for commercial purposes.

an essential role in the interfacial binding and activity of other PLA<sub>2</sub> isoforms.<sup>[14]</sup> Han et al. reported that tryptophan 31 in the binding surface of human group V PLA<sub>2</sub> was essential for membrane penetration of the enzyme.<sup>[15]</sup> Hence, a mutation of tryptophan 31 reduced enzyme activity 7-fold.<sup>[16]</sup> Notably, Beers et al. reported that the addition of only a single tryptophan to the membrane binding surface of human group IIA significantly enhanced the enzyme activity.<sup>[17]</sup> PLA<sub>2</sub> enzymes which contain the tryptophan residue in the interfacial binding surface are reported to display the highest activity toward neutral phospholipid substrates.<sup>[18]</sup> Gaspar et al. found that the non-steroidal anti-inflammatory drugs (NSAIDs) inhibit PLA<sub>2</sub> activity due to the disturbance of the enzyme binding efficiency to the membrane, possibly by shielding the tryptophan residues of the enzyme.<sup>[19]</sup> Based on that, we considered the destruction of the tryptophan-lipid interactions beneficial for the enzyme inhibition.

It is reported that the indole ring of the tryptophan has efficient interactions with the membrane's interfacial region.<sup>[20]</sup> We aimed to determine if the cleavage of the indole ring leads to the loss of effective enzyme-membrane binding. Tryptophan oxidation has been shown to be responsible for the opening of the indole ring.<sup>[21]</sup> To this end, cold physical plasma (CPP) was used as a source of reactive oxygen and nitrogen species (RONS) for tryptophan oxidation. CPP is a promising medical tool, which has been widely studied in different fields of medicine, such as cancer cell treatment, blood coagulation, wound healing, and skin disease treatment.<sup>[22]</sup> CPP is a body-temperature ionized gas produced at atmospheric pressure by applying energy to neutral gases.<sup>[23]</sup> CPP produces a mixture of active agents, including free charged particles, radicals, RONS, UV radiation, and electromagnetic fields.<sup>[24]</sup> It is assumed that plasma generated RONS, such as hydrogen peroxide (H<sub>2</sub>O<sub>2</sub>), ozone (O<sub>3</sub>), hydroxyl radical (\*OH), superoxide (\*O<sub>2</sub><sup>-</sup>), singlet oxygen (<sup>1</sup>O<sub>2</sub>), atomic oxygen (O), peroxyxynitrite (ONOO<sup>-</sup>), and nitric oxide (\*NO) are the critical elements in the above mentioned medical applications of CPPs.<sup>[25]</sup>

Herein, we report the effective inhibition of bee venom PLA<sub>2</sub> by direct plasma treatment. The choice of enzyme was based on the existence of a tryptophan residue on its interfacial region. Supported lipid bilayers (SLBs) were prepared on the surface of a gold electrode, and the activity of the wild-type and plasma-treated enzymes to cleave the SLBs was monitored by electrochemical techniques. Moreover, a detailed analysis of the effect of plasma-produced RONS on the enzyme peptide chain was performed using high-resolution liquid chromatography-tandem mass spectrometry (HR-LC-MS). Finally, the impact of tryptophan oxidation on the enzyme-lipid interactions was identified by molecular dynamics (MD) simulation and molecular docking studies.

## Results and Discussion

### Electrochemical studies to access the activity of PLA<sub>2</sub>

To study the PLA<sub>2</sub> activity to cleave the lipids, lipid bilayers from phosphoethanolamine (PE) and phosphatidylserine (PS) with ratio of PE:PS (70%:30%) were transferred onto the gold electrode surface by Langmuir-Blodgett and Langmuir-Schaefer deposition techniques. Optimum deposition pressure was assessed at 38 mN m<sup>-1</sup>, where significant changes in the plot of surface pressure as a function of area per lipid molecule ( $\pi$ -A isotherm) were observed. It is possible to decrease the bilayer thickness by lowering the deposition pressure. As a result, thicker bilayers will be transferred at higher deposition pressures.<sup>[26]</sup>

Electrochemical measurements were performed to confirm the successful transfer of the lipid bilayer to the electrode surface. As shown in Figure 1, the cyclic voltammogram (CV) and differential pulse voltammogram (DPV) of [Fe(CN)<sub>6</sub>]<sup>3-/4-</sup> as the redox probe, in the case of gold supported lipid bilayer had no significant peak current. This indicated that the gold electrode surface was covered with the lipid bilayer and the barrier properties of the transferred lipid bilayer were blocking the probe's access to the electrode surface. The enzymatic activity of PLA<sub>2</sub> to cleave the lipid bilayer was studied by injecting 10<sup>-4</sup> mg mL<sup>-1</sup> of the enzyme into the electrochemical cell containing the gold supported lipid bilayer working electrode. It is reported that the bee venom PLA<sub>2</sub> molecule is Ca<sup>2+</sup> dependent and highly basic (pI = 10.5 ± 1.0), which its

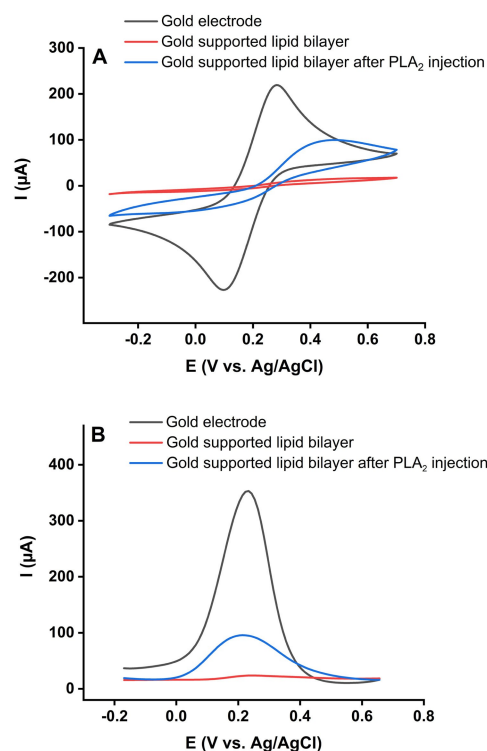


**Figure 1.** CVs (A) and DPVs (B) of the gold electrode, and gold supported lipid bilayer electrodes before and after injection of PLA<sub>2</sub> enzyme.

optimal activity occurs at alkaline pH.<sup>[27]</sup> Based on that, measurements were performed in Tris buffer (pH 8.9) containing 5 mM CaCl<sub>2</sub>.

The ability of the enzyme to hydrolyze the phospholipids damaged the lipid bilayer. It led to the gold electrode surface being more accessible for the redox probe, facilitating electron transfer between the probe and the electrode. As a result, the observed increase in the current and area of the DPV and CV peaks of [Fe(CN)<sub>6</sub>]<sup>3-/4-</sup> (Figure 1) after two hours was related to PLA<sub>2</sub> activity.

Balashov et al. have visualized the degradation of lipid bilayer due to the action of PLA<sub>2</sub> by atomic force microscopy. They found that hydrolysis of the lipid bilayer is initiated at specific regions where traces of structural bilayer defects or holes are distinguished or depressions in the bilayer have been identified. After PLA<sub>2</sub> injection, the existing structural defects were enlarged, and new holes appeared.<sup>[28]</sup>

The changes in lipid bilayer permeability after injection of PLA<sub>2</sub> to the electrochemical cell were calculated based on Equation (1).

$$\% \text{ Changes in permeability} = [(A_1 - A_2)/A_3] \times 100 \quad (1)$$

A<sub>1</sub>, A<sub>2</sub> and, A<sub>3</sub> were the area of the DPV curves of 10 mM [Fe(CN)<sub>6</sub>]<sup>3-/4-</sup> for gold supported lipid bilayer after two hours of PLA<sub>2</sub> injection, gold supported lipid bilayer, and gold electrode, respectively.

The effect of plasma treatment on the activity of the PLA<sub>2</sub> enzyme was investigated (Figure 2). A solution of 60 s Ar plasma-treated PLA<sub>2</sub> was added to the electrochemical cell containing a gold supported lipid bilayer working electrode. Interestingly, we found that lipid bilayer permeability changes were negligible (Figure 2A), which illustrated that the plasma-treated enzyme was no longer able to hydrolyze the phospholipids. To better understand the plasma-mediated enzyme inhibition, Tris buffer (pH 7.4) was exposed to Ar plasma, and the PLA<sub>2</sub> enzyme was added immediately after. The results of which demonstrated that this 'indirectly'-treated enzyme cleaved the lipid bilayer to increase its permeability: as such, indirect plasma treatment could not inhibit the enzyme activity. We concluded that short-lived reactive species from plasma were responsible for the observed enzyme inactivation, and the responsible agents for enzyme inactivation were lost in indirect treatment. Accordingly, the concentrations of deposited reactive species during 60 s Ar plasma treatment were quantified (Figure S2). We found •OH and <sup>1</sup>O<sub>2</sub> as short-lived and H<sub>2</sub>O<sub>2</sub>, nitrite (NO<sub>2</sub><sup>-</sup>), and nitrate (NO<sub>3</sub><sup>-</sup>) as long-lived plasma-produced reactive species in our measurement. Further experiments were conducted by adding a similar amount of identified long-lived reactive species to the PLA<sub>2</sub> solution. The obtained results are shown in Figure 2A, which indicated that none of these species were able to inactivate the enzyme.

<sup>1</sup>O<sub>2</sub> was one of the short-lived reactive species found only within direct plasma treatment (Figure S2) and is reported to be related to the anti-tumor effects of CPP.<sup>[29]</sup> Bauer et al. introduced 2 mM of histidine as a standard concentration of <sup>1</sup>O<sub>2</sub> scavenger.<sup>[30]</sup> To assess the effect of <sup>1</sup>O<sub>2</sub>, histidine was added to

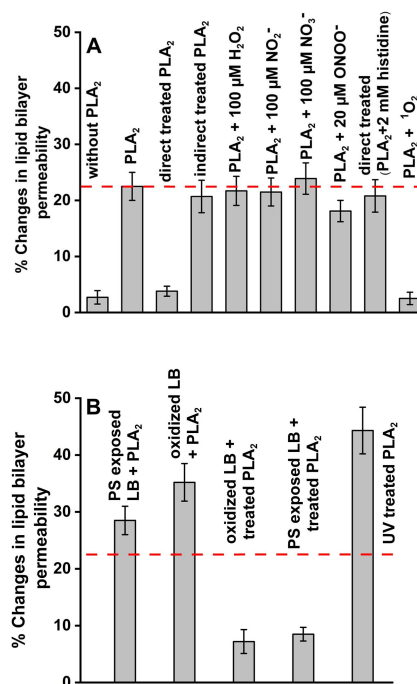


**Figure 2.** The changes in the PE: PS (70%: 30%) lipid bilayer (LB) permeability after incubation of bilayer with PLA<sub>2</sub> enzyme for 2 h (A). The changes in the lipid bilayer permeability after incubation of PE: PS lipid bilayers with different physical properties with PLA<sub>2</sub> for 2 h (B). The dashed red line indicated the activity of wild-type PLA<sub>2</sub> to cleave PE: PS (70%: 30%) lipid bilayer.

the PLA<sub>2</sub> solution during direct plasma treatment. It was found that in the presence of histidine, the direct plasma-induced abrogation was abolished. This suggested <sup>1</sup>O<sub>2</sub> to be the responsible agent for the enzyme inactivation. To verify the role of <sup>1</sup>O<sub>2</sub> in enzyme inhibition, a solution of PLA<sub>2</sub> in D<sub>2</sub>O was irradiated in the presence of 10 μM of rose bengal as photosensitizer with continuous oxygenation. Then, the appropriate amount of the irradiated enzyme was injected in the electrochemical cell containing gold supported lipid bilayer to have 10<sup>-4</sup> mg mL<sup>-1</sup> PLA<sub>2</sub>. After two hours, the changes in the permeability of the lipid bilayer were monitored. We found that the irradiated enzyme was inactivated and was not able to cleave the phospholipids. The control experiment was repeated similarly by mixing PLA<sub>2</sub> and rose bengal in D<sub>2</sub>O without irradiation. In the control experiment, the enzyme was able to cleave the bilayer and increase the permeability. These results confirm our suggestion that <sup>1</sup>O<sub>2</sub> is involved in the inactivation of the enzyme by plasma treatment. Moreover, the effect of substrate physical properties on the PLA<sub>2</sub> activity was investigated and is shown in Figure 2B. The obtained results indicated that wild-type PLA<sub>2</sub> had a higher activity for cleaving oxidized and PS exposed lipid bilayers (PE: PS (50%: 50%)) due to the altered structure of the membrane, which facilitated adsorption and access of the PLA<sub>2</sub> to the sn-2 ester bond of the phospholipids.<sup>[31]</sup> However, cleavage of the oxidized and PS exposed membranes by treated PLA<sub>2</sub> was sluggish. Furthermore, the impact of UV radiation from the plasma on the

activity of PLA<sub>2</sub> was investigated. The enzyme was treated in a chamber with an MgF<sub>2</sub> window to eliminate the effects of plasma-generated RONS and ensure only UV radiation can affect the enzyme. As shown in Figure 2B, the UV radiation increases the enzyme activity of lipid cleavage and as such is unlikely to be an influential factor in enzyme inhibition.

### Dynamic light scattering (DLS) and circular dichroism (CD)-spectroscopy measurements

DLS was performed to analyze possible enzyme degradation or aggregation by investigating any changes in size and heterogeneity of the enzyme after plasma treatment. Comparing the correlograms of PLA<sub>2</sub>, there were no significant changes in the light scatter decay time (Figure 3A) and the total area under the curve (AUC) (Figure 3B) for the enzyme after plasma treatment. The high polydispersity index (wild-type=0.85, plasma-treated=0.87) suggested a significant level of heterogeneity that did not change following plasma treatment. Additionally, the size of the enzyme before and after plasma treatment was measured as 4.97±0.85 nm (wild-type) and 4.58±0.72 nm (plasma-treated) (Figure 3C), which revealed no notable changes in diameter after plasma treatment. Collectively, these findings suggest no enzyme degradation or aggregation as a result of plasma treatment.

Consequently, we performed CD-spectroscopy analyses to track the changes in the secondary structure of the enzyme that may appear after plasma treatment. For this purpose, the CD spectra of the PLA<sub>2</sub> enzyme before and after plasma treatment with the Tris buffer spectrum used as the control measurement were recorded. As is shown in Figure 3D, the enzyme  $\alpha$ -helix is depicted in the CD-spectra without considerable changes. Assuming a constant enzyme concentration in both measurements, no significant differences appeared in the enzyme's secondary structure after plasma treatment.

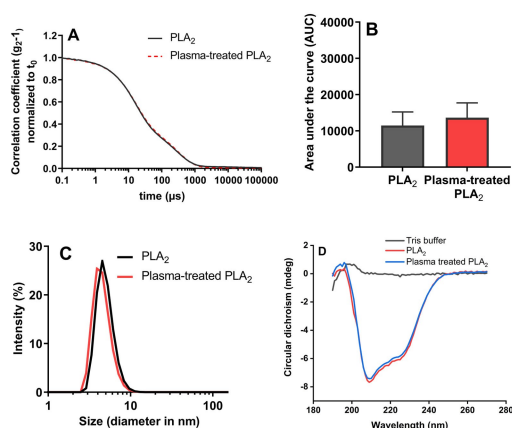


**Figure 3.** Correlation coefficient (A), AUC (B), and the size (C) of untreated and plasma-treated PLA<sub>2</sub> in Tris buffer (pH 7.4) measured by DLS (n=3), and CD spectra of Tris buffer (pH 7.4) and PLA<sub>2</sub> enzyme before and after plasma treatment (D) (n=2).

### HR-LC-MS analysis

The inactivation of the plasma-treated PLA<sub>2</sub> prompted us to analyze the oxidative modifications of the enzyme induced by RONS using HR-LC-MS. The coverage of the protein sequence was more than 90% before filtering the peptide spectrum matches with Byonic and delta mod score and 75% after filtering. The comparison of the chromatograms revealed that cysteine and methionine, as very reactive amino acids,<sup>[21e,32]</sup> did not show significant oxidative modifications after plasma treatment. However, tryptophan 128 at the exterior of the enzyme appeared as a hot spot. A detailed view of the RONS-induced oxidative modification sites found in the amino acid sequence of the enzyme after plasma treatment and the relative amount of each modification compared to the total number of modifications is shown in Figure 4. Obviously, among all modifications, tryptophan 128 dioxidation constituted more than 25% of all the identified modifications. This number indicated the high susceptibility of tryptophan to dioxidation, possibly due to the oxidation by <sup>1</sup>O<sub>2</sub> produced from plasma. The origin of other detected plasma-induced modifications of amino acids was studied extensively.<sup>[33]</sup>

Dioxidation of tryptophan resulted in the formation of different products.<sup>[34]</sup> Li et al. have studied the chemical basis of tryptophan oxidation using an Ar plasma jet.<sup>[35]</sup> In addressing this issue, they fully characterized each tryptophan-derived product using LC-MS<sup>2</sup>. They demonstrated that the plasma-induced oxidation of tryptophan gave rise to a mixture of hydroxyl derivatives and hydroperoxides, which were decom-

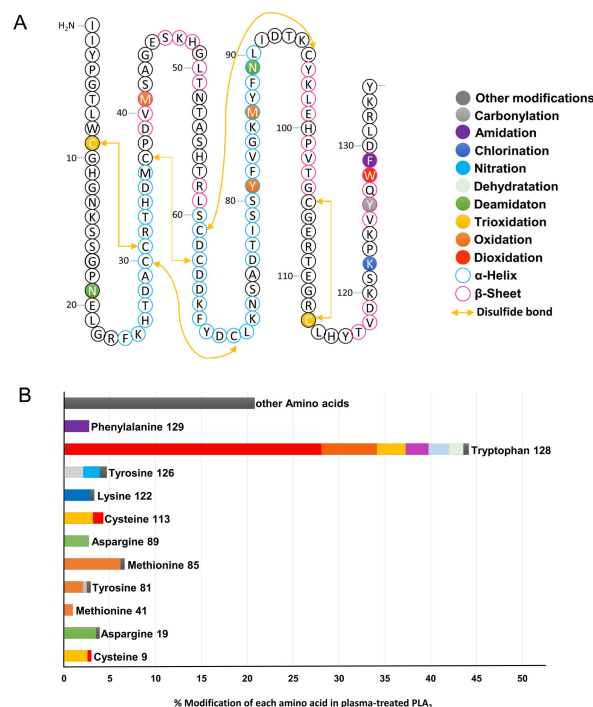


**Figure 4.** The complete amino acid sequence of PLA<sub>2</sub> with the specific location of each identified RONS-induced modification (A), and the relative amount of each amino acid modification in plasma-treated PLA<sub>2</sub> compared to the total number of modifications (B).

posed into N-formylkynurenine (NFK) under physiological conditions. Furthermore, they proposed a mechanism for the tryptophan reaction with the plasma-generated RONS, which introduced NFK as the final product of tryptophan oxidation by the Ar plasma jet. Moreover, Ronsein et al. have studied the mechanism of tryptophan oxidation by  $^1\text{O}_2$ .<sup>[21b]</sup> They characterized two cis- and trans-tryptophan hydroperoxide (WOOH) isomers as the major tryptophan oxidation products. They have shown that WOOHs were highly unstable and rapidly decomposed under heating or basification, leading to the formation of NFK. A similar mechanism was proposed by Gracanin et al. for tryptophan oxidation to NFK.<sup>[36]</sup> As plasma is a body-temperature ionized gas, and the treatment was done at slightly basic solutions (pH 7.4) and based on the UV absorption spectra (Figure S5), we assigned NFK as the major product of tryptophan dioxidation and the main oxidative product in the plasma-treated PLA<sub>2</sub> sequence.

The oxidation of tryptophan to NFK in proteins has been known. Kuroda et al. found that inactivation of lysozyme occurred only when one specific tryptophan residue was oxidized to NFK.<sup>[37]</sup> It was the first evidence that oxidation of a particular tryptophan residue can impair enzyme activity. They reported this oxidative inactivation is accompanied by the loss of the ability of lysozyme to form an enzyme-substrate complex. Moreover, tryptophan dioxidation to NFK has been detected in a variety of other proteins, including mitochondrial ATP synthase,<sup>[38]</sup> photosystem II subunits,<sup>[39]</sup> apolipoprotein B-100,<sup>[40]</sup> myoglobin,<sup>[41]</sup> aconitase-2 (mitochondria),<sup>[42]</sup> frataxin,<sup>[43]</sup> troponin I and actin.<sup>[44]</sup> Furthermore, Kasson et al. introduced NFK as a new marker identify ROS generation sites in photosystem II and other proteins.<sup>[45]</sup>

It is known that the interactions of the tryptophan indole ring with biomembranes are highly remarkable in their solvation.<sup>[20,46]</sup> As a result, tryptophan dioxidation and the indole ring-opening can prevent membrane proteins from efficiently anchoring into the lipid bilayer, which leads to enzyme inactivation. To prove our hypothesis, MD simulation and molecular docking were done to measure the interactions between wild-type PLA<sub>2</sub> containing tryptophan 128 residue and plasma-treated PLA<sub>2</sub> with the NFK group and a PE lipid.

### MD simulation

To further highlight that tryptophan dioxidation and NFK formation had no effect on the size and structure of the enzyme, but only altered the interactions with phospholipids, MD simulation was applied. For this purpose, structures and the surface electrostatic potentials indicating the positively and negatively charged regions for the wild-type and plasma-treated PLA<sub>2</sub> were generated with PyMol and APBS and are compared in Figure 5. As is shown, there were no significant changes in the enzyme's structure and size after plasma treatment; especially in the active site of the enzyme, supports the finding of the obtained DLS and CD-spectroscopy experimental data. The most apparent structural change was observed in the region where tryptophan 128, tyrosine 126, and

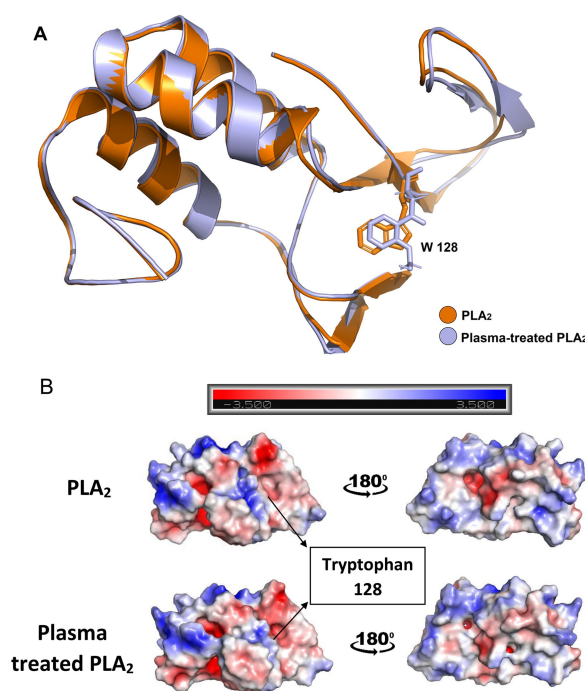


**Figure 5.** Structural alignments (A) and surface electrostatic potentials (blue for positively charged, red for negatively charged), before and after rotation by 180° about the vertical axis (B) for wild-type and plasma-treated PLA<sub>2</sub>.

phenylalanine 129 were modified. Moreover, root-mean-square-deviation (RMSD) for untreated against plasma-treated PLA<sub>2</sub> was calculated as 0.585. This small RMSD suggests only partial differences between the structure of enzyme before and after plasma treatment.

As mentioned, tryptophan plays an essential role in the binding of membrane enzymes. In this regard, FTMap<sup>[47]</sup> was performed to identify if tryptophan 128 could be a hotspot for different ligands. It was found that tryptophan 128 is able to establish hydrogen bonds with 2.46% ligands (Figure S6), which was a significant percentage for the outer region of the enzyme active site. Hydrogen bonds and electrostatic- $\pi$  interactions are essential for indole solvation, and these interactions are responsible for tryptophan's role in anchoring proteins into the membrane.<sup>[46]</sup> As a result, any changes in the indole ring structure due to plasma treatment could affect tryptophan's ability to bond with the membrane. As such, molecular docking was performed to simulate the interactions between PE lipid and wild-type or plasma-treated PLA<sub>2</sub> with tryptophan or NFK residues, respectively.

The molecular docking results indicate that PE lipids can establish two groups of hydrogen bonding via its carbonyl groups with tryptophan 128 of wild-type PLA<sub>2</sub>. The first hydrogen bonding was between the lipid carbonyl group and NH<sub>2</sub> of tryptophan 128, which had an angle of 14.5 degrees to the x-axis, and 143.8 degrees to the y-axis at a distance of 3.0 Å. The other hydrogen bond formation was between the N atom of the tryptophan 128 indole ring and the second carbonyl group of PE, with an angle of 17.9 degrees to the x-axis and 116.8

degrees to the y-axis at a distance of 2.8 Å (Figure 6A and B). After plasma treatment and dioxidation of tryptophan, these hydrogen bond and the other electrostatic- $\pi$  interactions of tryptophan 128 with phospholipid were eliminated (Figure 6C and D). Dioxidation of tryptophan and opening of the indole ring decreased the total interactions between the phospholipid and the enzyme. The enzyme's affinity for ligand binding was calculated as  $-4.3 \text{ kcal mol}^{-1}$  (docking score) for PLA<sub>2</sub>, which was reduced to  $-3.4 \text{ kcal mol}^{-1}$  after plasma treatment. The molecular docking results indicated that in the case of plasma-treated PLA<sub>2</sub>, the absence of sufficient interactions between the enzyme and lipid membrane prevented enzyme localization in the lipid bilayer, which resulted in the inactivation of the enzyme.

Kubiak et al. studied the products of bovine eye lens protein gB-crystallin (GCS) oxidation by MD modeling.<sup>[48]</sup> They induced mutations at tryptophan residues converting them into NFK. According to quantum chemical calculations, they found the rearrangement of the charge distribution in the tryptophan moiety after its oxidation to NFK is localized in the opened indole ring. They demonstrated the increased local electric dipole moment of the NFK residue decreased the hydrophobicity of the molecule. Furthermore, they reported the NFK residue significantly more polar than tryptophan. Thus, under favorable conditions, new hydrogen bonds with water were created. They presented a snapshot from the GCS and NFK trajectories, showing that NFK penetrated the water further than tryptophan. Considering their results, oxidation of tryptophan to NFK was decreasing the lipophilicity of the treated enzyme. Thus, the plasma-treated enzyme had less affinity to form hydrogen bonds with phospholipids, leading to the loss of efficient interactions between the enzyme and phospholipids and enzyme inactivation. This could represent a novel treatment strategy for many diseases that involve PLA<sub>2</sub> over-expression.

## Conclusion

In this study, we demonstrated that the plasma-produced <sup>1</sup>O<sub>2</sub> led to the efficient inactivation of the PLA<sub>2</sub> enzyme, which is highly desirable due to its increased activity in many diseases. We verified that the dioxidation of interfacial tryptophan 128 residue to NFK led to the decay of functional interactions between the enzyme and phospholipid, preventing the enzyme from anchoring in the membrane and consequently inhibited the enzyme efficiently. The introduced inhibition mechanism is not limited to the PLA<sub>2</sub> enzyme, but can be extended to those proteins in which interfacial tryptophan plays a role in their membrane anchoring and functionality. Influenza virus haemagglutinin,<sup>[49]</sup> Ebola virus matrix protein,<sup>[50]</sup> multidrug resistance protein 1,<sup>[51]</sup> and Escherichia coli  $\alpha$ -Hemolysin<sup>[52]</sup> are only a few examples in which tryptophan residues are known to be required for their stabilizing and proper function in cells. This study deepens our knowledge of the structure-function relationship of the PLA<sub>2</sub> enzyme and introduces the possibility of using this inactivation strategy based on pro-oxidant

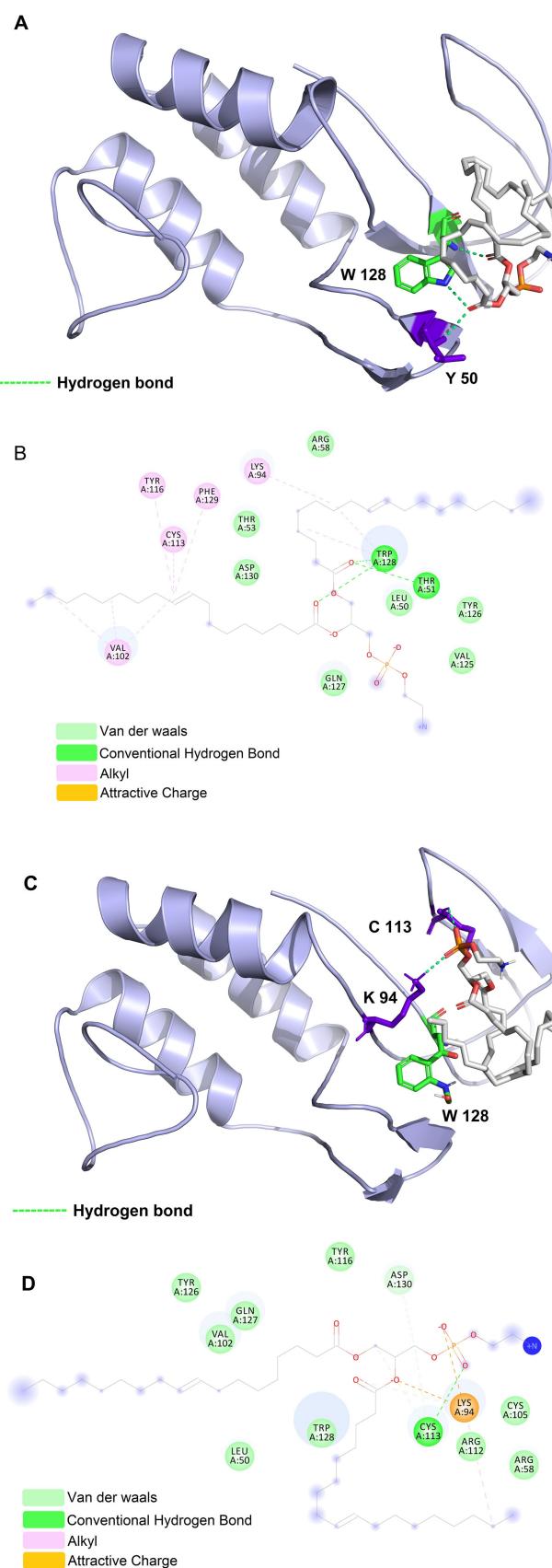


**Figure 6.** 3D and 2D interactions of PLA<sub>2</sub> and PE lipid before (A and B) and after (C and D) plasma treatment. Abbreviations for amino acids: W: tryptophan, Y: tyrosine, C: cysteine, K: lysine.

therapies for all the proteins in which tryptophan has a role in their membrane anchoring and functionality.

## Experimental Section

### Reagents

1,2-dioleoyl-sn-glycero-3-phosphoethanolamine (18:1 ( $\Delta 9$ -Cis) PE (DOPE)) and 1,2-dioleoyl-sn-glycero-3-phospho-L-serine (sodium salt) (18:1 PS (DOPS)) were from Avanti Polar Lipids and purchased from Otto Nordwald (Otto Nordwald GmbH, Germany) and used without further purification. Chloroform and ethanol were HPLC grade from Carl Roth (Carl Roth GmbH+Co. KG, Germany). Methanol (99.95%) was from Th. Geyer (Th. Geyer GmbH & Co. KG, Germany). Phospholipase A<sub>2</sub> from honey bee venom (Apis mellifera, UniProt P00630), rose bengal, potassium hexacyanoferrate(II) trihydrate, potassium hexacyanoferrate(III), and hydrogen peroxide (30% w/w) were purchased from Sigma-Aldrich (Sigma-Aldrich Chemie GmbH, Germany). Peroxynitrite was from Merck (Merck Chemicals GmbH, Germany). Water used for cleaning and measurements was purified with ultrapure MilliQ water (Milli-Q® Merck KGaA, Germany). All other reagents were of analytical grade and used without further purification.

### Preparation of gold supported lipid bilayer

To prepare the gold-supported lipid bilayers, Langmuir-Blodgett (LB) and Langmuir-Schaefer (LS) deposition techniques were applied for the transfer of the first and second lipid monolayers onto the Au(111) (arrandee metal GmbH+Co. KG, Germany) substrates, respectively. For this purpose, surface pressure-area isotherms were recorded using a Langmuir trough (KSV NIMA, LOT-QuantumDesign GmbH, Germany). The Au (111) substrate was flame-annealed and cleaned in piranha solution (3:1 mixture of concentrated sulfuric acid and 30% hydrogen peroxide solution) before being transferred into the trough.<sup>[53]</sup> A sufficient quantity of 1 mg mL<sup>-1</sup> lipid solution was dispersed onto the surface of the water subphase in a dropwise manner. The lipid solvent was allowed to evaporate for 15 min, and then the barriers were closed to obtain the target pressure of 38 mNm<sup>-1</sup>. The Au substrate was raised vertically through the monolayer film at a speed of 2 mm min<sup>-1</sup>, while the pressure was maintained at the target pressure and then dried in argon for 30 min. A transfer ratio of 1.0 ± 0.1 was accepted as a successful transfer of the lipid to the substrate. To transfer the second monolayer, the Langmuir-Schaefer (horizontal dip) was performed at a speed of 0.5 mm min<sup>-1</sup>. The Au substrate-supported lipid bilayer was placed immediately into the electrochemical cell.

### Electrochemical measurements

Electrochemical measurements were carried out using a potentiostat AUTOLAB PGSTAT302 N (Deutsche METROHM GmbH & Co. KG, Germany) electrochemical system. All experiments were performed in a three-electrode system consisting of a leakless Ag/AgCl miniature reference electrode and a platinum wire auxiliary electrode (eDAQ Europe, Poland), and a gold substrate supported lipid bilayer as the working electrode. DPVs and CVs were recorded in a solution of 10 mM [Fe(CN)<sub>6</sub>]<sup>3-/4-</sup> in Tris buffer [0.010 M Tris (pH 8.9), 0.150 M NaCl, 0.005 M CaCl<sub>2</sub>].

### CPP treatment

The kINPen09 (Neoplas tools GmbH, Germany) was used as a well-characterized plasma source<sup>[54]</sup> running at 1.1 W and a frequency of 1 MHz. Argon was used as feed gas at a flux of 3.0 standard liters per minute (slm). Volumes of 750  $\mu$ L of PLA<sub>2</sub> enzyme in Tris buffer [0.010 M Tris (pH 7.4), 0.150 M NaCl, 0.005 M CaCl<sub>2</sub>] were treated with the kINPen at a distance of 9 mm between the jet nozzle and the sample surface for 60 seconds.

### Singlet oxygen generation

Samples of 0.01 mg mL<sup>-1</sup> PLA<sub>2</sub> enzyme in D<sub>2</sub>O were irradiated for 30 minutes in the presence of 10  $\mu$ M of rose bengal as photosensitizer with PL201 compact laser module 520 nm wavelength (Thorlabs GmbH, Germany) with continuous oxygenation.

### DLS measurements

Samples of untreated and plasma-treated PLA<sub>2</sub> (1 mg mL<sup>-1</sup>) in Tris buffer (pH 7.4) were loaded in low-volume disposal cuvettes (ZEN0040). Spectra were recorded using a ZS90 dynamic light scattering device (Malvern Instruments, UK) equipped with a helium-neon laser light source (632 nm). The samples were measured at 25 °C, with an equilibration time of 120 seconds. Attenuator was set to 9, backscatter angled detection was performed at 173° with a scattering collection angle of 147.7°. Measurement was performed once in three technical replicates, with a measurement duration of 25.2 sec (1.68 sec per run) for each replicate. Data were evaluated with ZS XPLORER Software 1.3.0.140 and GraphPad prism 9.0.2.

### CD-spectroscopy

Circular dichroism data were monitored with a Chirascan CD spectrometer (Applied Photophysics, UK) combined with a temperature controller (Quantum Northwest, USA). Each measurement was done with samples in a concentration of 25  $\mu$ g mL<sup>-1</sup> diluted in Tris buffer (pH 7.4) and loaded in 5 mm-pathlength cuvettes (Hellma Analytics, Germany). CD spectra were recorded at 25 °C in the range of 190 to 270 nm with a bandwidth of 1.0 nm, a scanning time of 1.5 s per point, and five repetitions. All spectra were blank corrected and repeated at least two times.

### HR-LC-MS measurements and data analysis

The PLA<sub>2</sub> samples were heated for 10 min to 95 °C. After cooling down to room temperature, the protein was digested with trypsin with an enzyme to protein ratio of 1:25 for 2 h at 37 °C. After digestion, the peptides were ready for measurement by HR-LC-MS. The peptides were analyzed on an Orbitrap Exploris 480 mass spectrometer (Thermo Scientific, Germany) coupled to an UltiMate 3000 RSLCnano UHPLC system (Thermo Scientific, Germany). Peptides were loaded on a trap column (Acclaim PepMap100 C18 material, 5  $\mu$ M 0.1 × 20 mm, Thermo Fisher) with a flow rate of 5  $\mu$ L per minute for 6 minutes. The loaded peptides were resolved at 300 nL min<sup>-1</sup> flow rate using a linear gradient of 4 to 45% solvent B (0.1% acetic acid in 95% acetonitrile) over 42 minutes on an analytical column (150 mm × 75  $\mu$ m, 2.0  $\mu$ m particle size, Thermo Fisher Scientific). Attached was an EASY-Spray ion source operated at 1.9 kV voltage, and the temperature was 250 °C, with a stainless steel emitter.

Mass spectrometry analysis was carried out with the peptide application mode peptide and in a data-dependent manner with a

full scan range of 350 to 1200 m/z with top N where N was set to 15 most abundant ions. Both MS and ddMS<sup>2</sup> were measured using an Orbitrap mass analyzer. Full MS scans were measured with a resolution of 120,000 at 200 m/z. Precursor ions were fragmented using fixed normalized higher-energy collisional dissociation (HCD) collision of 30% and detected at a mass resolution of 15,000 at m/z 200. Normalized Automatic gain control (AGC) target for full MS was set to 300% (3e6 ions), and for MS<sup>2</sup> was set to standard with an automatic maximum ion injection time for full MS and 50 ms for ddMS<sup>2</sup>. Dynamic exclusion was set to 30 seconds, and singly charged ions were excluded. The raw data analysis to identify the peptides and the oxidative modifications was performed with the Proteome Discoverer 2.4.1.15 software (Thermo Fisher Scientific) using Byonic (Protein Metrics)<sup>[55]</sup> Version 3.8 as a plug-in tool. The peptide spectrum matches were filtered via Byonic score of 250 and delta mod score of 5. A list of expected oxidative modifications was used to screen and detect the modified peptides in Byonic (Table S2) can be found in the supplemented information of the paper.

### MD simulation

MD simulation and molecular docking were applied to investigate the structure of PLA<sub>2</sub> and the interactions between tryptophan 128 residue of wild-type and plasma-treated PLA<sub>2</sub> and PE lipid. MD simulation was performed with GROMACS<sup>[56]</sup> program package (version 5.0) OPLS-AA/L all-atom force field. The coordinate file of PLA<sub>2</sub> was obtained from the protein data bank (PDB ID: 1POC). The structure of PLA<sub>2</sub> was placed in the simulation box, and the box type was defined as a cube with a size of 5.5 nm. The box was filled with water molecules (the SPC water model) surrounding PLA<sub>2</sub>, sodium ions were added to the system. Afterward, the energy of the system was minimized. Eventually, a 100 ps equilibration run was performed employing the NVT ensemble (i.e., a system with a constant number of particles N, volume V and temperature T). Finally, a 100 ns production run was accomplished using NPT dynamics (i.e., a system with a constant number of particles N, pressure P, and temperature T). The reference pressure was set to 1 bar. The calculated values were not identical for wild-type and plasma-treated PLA<sub>2</sub>, and the treated enzyme showed less stability.

Molecular docking was performed by AutoDock Vina.<sup>[57]</sup> The model mentioned above was used as the target, and PE was obtained from PubChem<sup>[58]</sup> web server as the ligand. For docking, tryptophan 128 was chosen as the center of the grid box. According to affinity (kcal mol<sup>-1</sup>) and root-mean-square-deviation, which were given by AutoDock Vina, the best model for wild-type PLA<sub>2</sub> was selected. The interactions between untreated PLA<sub>2</sub> and PE ligand were analyzed using AutoDockTools-1.5.6 and Discovery Studio.<sup>[59]</sup> First, all the modifications detected by HR-LC-MS were applied to the wild-type PLA<sub>2</sub> using Avogadro<sup>[60]</sup> software. Afterward, energy minimization was performed to optimize the modified structure using the steepest descent algorithm. After that, according to the study done by Kubiak et al.,<sup>[48]</sup> angles and distances were investigated for tryptophan. Finally, the mentioned experiments were repeated to study the effect of modifications on the structure and interactions of treated PLA<sub>2</sub>. Subsequently, the best model for the plasma-treated PLA<sub>2</sub> was selected, and by PyMOL,<sup>[61]</sup> the structures of wild-type and plasma-treated PLA<sub>2</sub> were compared.

### Acknowledgements

The authors are grateful to Johanna Striesow for the mass analysis of lipid samples and Dr. Nicholas McKitterick for

proofreading the article. We also thank Lukas Schulig for valuable comments on molecular dynamics simulation. This work is funded by the German Federal Ministry of Education and Research (BMBF) (grant numbers 03Z22DN12 and 03Z22Di1). Open Access funding enabled and organized by Projekt DEAL.

### Conflict of Interest

The authors declare no conflict of interest.

**Keywords:** cold physical plasma · enzyme inhibition · plasma chemistry · protein modifications · reactive oxygen and nitrogen species

- [1] E. A. Dennis, J. Cao, Y. H. Hsu, V. Magriotti, G. Kokotos, *Chem. Rev.* **2011**, *111*, 6130–6185.
- [2] E. Gendaszewska-Darmach, *Acta Biochim. Pol.* **2008**, *55*, 227–240.
- [3] a) J. Chen, L. Ye, Y. Sun, Y. Takada, *Med. Chem.* **2017**, *13*, 606–615; b) Z. Peng, Y. Chang, J. Fan, W. Ji, C. Su, *Cancer Lett.* **2021**, *497*, 165–177.
- [4] a) S. A. Knowliden, S. E. Hillman, T. J. Chapman, R. Patil, D. D. Miller, G. Tigyi, S. N. Georas, *Am. J. Respir. Cell Mol. Biol.* **2016**, *54*, 402–409; b) S. J. Kim, H. G. Moon, G. Y. Park, *Biochim. Biophys. Acta Mol. Cell Biol. Lipids* **2020**, *1865*, 8; c) N. G. Jendzjowsky, A. Roy, N. O. Barioni, M. M. Kelly, F. H. Y. Green, C. N. Wyatt, R. L. Pye, L. Tenorio-Lopes, R. J. A. Wilson, *Nat. Commun.* **2018**, *9*, 15.
- [5] a) A. Trotter, E. Anstadt, R. B. Clark, F. Nichols, A. Dwivedi, K. Aung, J. L. Cervantes, *Mult. Scler. Relat. Disord.* **2019**, *27*, 206–213; b) J. Soubhye, P. van Antwerpen, F. Dufresne, *Curr. Med. Chem.* **2018**, *25*, 2418–2447; c) N. C. Stoddard, J. Chun, *Biomol. Ther.* **2015**, *23*, 1–11.
- [6] a) R. Junqueira, Q. Cordeiro, I. Meira-Lima, W. F. Gattaz, H. Vallada, *Psychiatr. Genet.* **2004**, *14*, 157–160; b) S. Smesny, D. Kinder, I. Willhardt, T. Rosburg, A. Lasch, G. Berger, H. Sauer, *Biol. Psychiatry* **2005**, *57*, 399–405; c) X. Meng, C. Kou, Q. Yu, J. Shi, Y. Yu, *Psychiatry Res.* **2010**, *175*, 186–187; d) C. Y. Xu, X. H. Yang, L. Y. Sun, T. Q. Yang, C. Q. Cai, P. Wang, J. Jiang, Y. Qing, X. W. Hu, D. D. Wang, P. K. Wang, G. P. Cui, J. Zhang, Y. Li, J. Feng, C. X. Liu, C. L. Wan, *Psychiatry Res.* **2019**, *273*, 782–787.
- [7] H. Qasem, L. Al-Ayadhi, H. Al Dera, A. El-Ansary, *Lipids Health Dis.* **2017**, *16*.
- [8] a) I. Meira-Lima, D. Jardim, R. Junqueira, E. Ikenaga, H. Vallada, *Bipolar Disord.* **2003**, *5*, 295–299; b) M. V. Zanetti, R. Machado-Vieira, H. P. G. Joaquin, T. M. Chaim, M. H. Serpa, R. T. de Sousa, W. F. Gattaz, G. F. Busatto, L. L. Talib, *Biol. Psychiatry* **2016**, *79*, 2665–2675.
- [9] a) A. Nikolaou, M. G. Kokotou, S. Vasilikaki, G. Kokotos, *Biochim. Biophys. Acta Mol. Cell Biol. Lipids* **2019**, *1864*, 941–956; b) Q. Z. Zhang, R. H. Fang, W. W. Gao, L. F. Zhang, *Angew. Chem. Int. Ed.* **2020**, *6*.
- [10] A. S. Alekseeva, P. E. Volynsky, N. A. Krylov, V. P. Chernikov, E. L. Vodovozova, I. A. Boldyrev, *Biochim. Biophys. Acta Biomembr.* **2021**, *1863*, 10.
- [11] A. J. de Jesus, T. W. Allen, *Biochim. Biophys. Acta* **2013**, *1828*, 864–876.
- [12] C. C. Leslie, *J. Lipid Res.* **2015**, *56*, 1386–1402.
- [13] J. H. Evans, C. C. Leslie, *J. Biol. Chem.* **2004**, *279*, 6005–6016.
- [14] M. Gelb, W. Cho, D. Wilton, *Curr. Opin. Struct. Biol.* **1999**, *9*, 428–432.
- [15] S. K. Han, K. P. Kim, R. Koduri, L. Bittova, N. M. Munoz, A. R. Leff, D. C. Wilton, M. H. Gelb, W. Cho, *J. Biol. Chem.* **1999**, *274*, 11881–11888.
- [16] R. V. Stahelin, W. Cho, *Biochemistry* **2001**, *40*, 4672–4678.
- [17] S. A. Beers, A. G. Buckland, N. Giles, M. H. Gelb, D. C. Wilton, *Biochemistry* **2003**, *42*, 7326–7338.
- [18] a) S. Bezzine, J. G. Bollinger, A. G. Singer, S. L. Veatch, S. L. Keller, M. H. Gelb, *J. Biol. Chem.* **2002**, *277*, 48523–48534; b) O. G. Berg, M. H. Gelb, M.-D. Tsai, M. K. Jain, *Chem. Rev.* **2001**, *101*, 2613–2654.
- [19] D. Gaspar, M. Lucio, S. Rocha, J. Lima, S. Reis, *Chem. Phys. Lipids* **2011**, *164*, 292–299.
- [20] a) A. N. Ridder, S. Morein, J. G. Stam, A. Kuhn, B. de Kruijff, J. A. Killian, *Biochemistry* **2000**, *39*, 6521–6528; b) H. C. Gaede, W. M. Yau, K. Gawrisch, *J. Phys. Chem. B* **2005**, *109*, 13014–13023; c) K. E. Norman, H. Nymeyer, *Biophys. J.* **2006**, *91*, 2046–2054.

- [21] a) M. J. Davies, *Biochem. Biophys. Res. Commun.* **2003**, *305*, 761–770; b) G. E. Ronsein, M. C. B. Oliveira, S. Miyamoto, M. H. G. Medeiros, P. Di Mascio, *Chem. Res. Toxicol.* **2008**, *21*, 1271–1283; c) G. E. Ronsein, M. C. de Oliveira, M. H. de Medeiros, P. Di Mascio, *J. Am. Soc. Mass Spectrom.* **2009**, *20*, 188–197; d) J. E. Plowman, S. Deb-Choudhury, A. J. Grosvenor, J. M. Dyer, *Photochem. Photobiol. Sci.* **2013**, *12*, 1960–1967; e) G. Uchida, Y. Mino, T. Suzuki, J. I. Ikeda, T. Suzuki, K. Takenaka, Y. Setsuhara, *Sci. Rep.* **2019**, *9*, 6625.
- [22] a) M. L. Semmler, S. Bekeschus, M. Schafer, T. Bernhardt, T. Fischer, K. Witzke, C. Seebauer, H. Rebl, E. Grambow, B. Vollmar, J. B. Nebe, H. R. Metelmann, T. V. Woedtke, S. Emmert, L. Boeckmann, *Cancers* **2020**, *12*; b) S. Bekeschus, J. Brüggemeier, C. Hackbarth, T. von Woedtke, L.-I. Partecke, J. van der Linde, *Clin. Plasma Med.* **2017**, *7–8*, 58–65; c) O. Assadian, K. J. Ousey, G. Daeschlein, A. Kramer, C. Parker, J. Tanner, D. J. Leaper, *Int. Wound J.* **2019**, *16*, 103–111; d) T. Bernhardt, M. L. Semmler, M. Schäfer, S. Bekeschus, S. Emmert, L. Boeckmann, *Oxidative Medicine and Cellular Longevity* **2019**, *2019*, 3873928.
- [23] K. D. Weltmann, T. von Woedtke, *Plasma Phys. Controlled Fusion* **2017**, *59*, 014031.
- [24] a) T. von Woedtke, A. Schmidt, S. Bekeschus, K. Wende, K. D. Weltmann, *In vivo* **2019**, *33*, 1011–1026; b) A. Privat-Maldonado, A. Schmidt, A. Lin, K. D. Weltmann, K. Wende, A. Bogaerts, S. Bekeschus, *Oxid. Med. Cell. Longevity* **2019**, *2019*, 9062098.
- [25] a) D. Yan, J. H. Sherman, M. Keidar, *Oncotarget* **2016**; b) M. Keidar, *Phys. Plasmas* **2018**, *25*, 083504; c) X. Lu, M. Keidar, M. Laroussi, E. Choi, E. J. Szili, K. Ostrikov, *Mat. Sci. Eng. R.* **2019**, *138*, 36–59.
- [26] A. V. Hughes, S. J. Roser, M. Gerstenberg, A. Goldar, B. Stidder, R. Feidenhans'l, J. Bradshaw, *Langmuir* **2002**, *18*, 8161–8171.
- [27] R. A. Shipolini, G. L. Callewaert, R. C. Cottrell, S. Doonan, C. A. Vernon, B. E. Banks, *Eur. J. Biochem.* **1971**, *20*, 459–468.
- [28] K. Balashev, N. John DiNardo, T. H. Callisen, A. Svendsen, T. Bjornholm, *Biochim. Biophys. Acta* **2007**, *1768*, 90–99.
- [29] a) G. Bauer, D. B. Graves, *Plasma Processes Polym.* **2016**, *13*, 1157–1178; b) G. Bauer, *Anti-Cancer Agents Med. Chem.* **2018**, *18*, 784–804; c) G. Bauer, *IEEE Trans. Radiat. Plasma Med. Sci.* **2018**, *2*, 87–98.
- [30] G. Bauer, D. Sersenová, D. B. Graves, Z. Machala, *Sci. Rep.* **2019**, *9*, 14210.
- [31] a) J. J. van den Berg, J. A. Op den Kamp, B. H. Lubin, F. A. Kuypers, *Biochemistry* **1993**, *32*, 4962–4967; b) E. Gibbons, J. Nelson, L. Anderson, K. Brewer, S. Melchor, A. M. Judd, J. D. Bell, *Biochim. Biophys. Acta* **2013**, *1828*, 670–676.
- [32] a) G. Bruno, T. Heusler, J.-W. Lackmann, T. von Woedtke, K.-D. Weltmann, K. Wende, *Clin. Plasma Med.* **2019**, *14*, 100083; b) S. Wenske, J.-W. Lackmann, S. Bekeschus, K.-D. Weltmann, T. von Woedtke, K. Wende, *Biointerphases* **2020**, *15*.
- [33] a) E. Takai, T. Kitamura, J. Kuwabara, S. Ikawa, S. Yoshizawa, K. Shiraki, H. Kawasaki, R. Arakawa, K. Kitano, *J. Phys. D* **2014**, *47*, 285403; b) S. Wenske, J. W. Lackmann, L. M. Busch, S. Bekeschus, T. von Woedtke, K. Wende, *J. Appl. Phys.* **2021**, *129*; c) S. Wenske, J. W. Lackmann, S. Bekeschus, K. D. Weltmann, T. von Woedtke, K. Wende, *Biointerphases* **2020**, *15*, 061008; d) S. Jiang, L. Carroll, L. M. Rasmussen, M. J. Davies, *Redox Biol.* **2021**, *38*, 101822; e) S. Jiang, L. Carroll, M. Mariotti, P. Häggglund, M. J. Davies, *Redox Biol.* **2021**, *41*, 101874.
- [34] P. Di Mascio, G. R. Martinez, S. Miyamoto, G. E. Ronsein, M. H. G. Medeiros, J. Cadet, *Chem. Rev.* **2019**, *119*, 2043–2086.
- [35] X. Y. Li, Z. Q. Feng, S. C. Pu, Y. Yang, X. M. Shi, Z. Xu, *Plasma Chem. Plasma Process.* **2018**, *38*, 919–936.
- [36] M. Gracianin, C. L. Hawkins, D. I. Pattison, M. J. Davies, *Free Radical Biol. Med.* **2009**, *47*, 92–102.
- [37] M. Kuroda, F. Sakiyama, K. Narita, *J. Biochem.* **1975**, *78*, 641–651.
- [38] S. Rexroth, A. Poetsch, M. Rogner, A. Hamann, A. Werner, H. D. Osiewacz, E. R. Schafer, H. Seelert, N. A. Dencher, *Biochim. Biophys. Acta* **2012**, *1817*, 381–387.
- [39] a) T. M. Dreaden, J. Chen, S. Rexroth, B. A. Barry, *J. Biol. Chem.* **2011**, *286*, 22632–22641; b) T. M. D. Kasson, S. Rexroth, B. A. Barry, *PLoS One* **2012**, *7*; c) S. Rinalducci, N. Campostrini, P. Antonioli, P. G. Righetti, P. Roepstorff, L. Zolla, *J. Proteome Res.* **2005**, *4*, 2327–2337.
- [40] A. Gießauf, B. van Wickern, T. Simat, H. Steinhart, H. Esterbauer, *FEBS Lett.* **1996**, *389*, 136–140.
- [41] M. Ehrenshaft, S. O. Silva, I. Perdivara, P. Bilski, R. H. Sik, C. F. Chignell, K. B. Tomer, R. P. Mason, *Free Radical Biol. Med.* **2009**, *46*, 1260–1266.
- [42] C. Hunzinger, W. Wozny, G. P. Schwall, S. Poznanovic, W. Stegmann, H. Zengerling, R. Schoepf, K. Groebe, M. A. Cahill, H. D. Osiewacz, N. Jagemann, M. Bloch, N. A. Dencher, F. Krause, A. Schratzenholz, *J. Proteome Res.* **2006**, *5*, 625–633.
- [43] A. R. Correia, S. Y. Ow, P. C. Wright, C. M. Gomes, *Biochem. Biophys. Res. Commun.* **2009**, *390*, 1007–1011.
- [44] M. Fedorova, T. Todorovsky, N. Kuleva, R. Hoffmann, *Proteomics* **2010**, *10*, 2692–2700.
- [45] T. M. D. Kasson, B. A. Barry, *Photosynth. Res.* **2012**, *114*, 97–110.
- [46] A. J. Johnston, Y. R. Zhang, S. Busch, L. C. Pardo, S. Imberti, S. E. McLain, *J. Phys. Chem. B* **2015**, *119*, 5979–5987.
- [47] D. Kozakov, L. E. Grove, D. R. Hall, T. Bohnuud, S. E. Mottarella, L. Luo, B. Xia, D. Beglov, S. Vajda, *Nat. Protoc.* **2015**, *10*, 733–755.
- [48] K. Kubiak, M. Kowalska, W. Nowak, *J. Mol. Struct.: THEOCHEM* **2003**, *630*, 315–325.
- [49] N. Ogata, *J. Gen. Virol.* **2012**, *93*, 2558–2563.
- [50] K. A. Johnson, R. Pokhrel, M. R. Budicini, B. S. Gerstman, P. P. Chapagain, R. V. Stahelin, *Pathogens* **2020**, *9*, 402.
- [51] K. Ito, S. L. Olsen, W. Qiu, R. G. Deeley, S. P. Cole, *J. Biol. Chem.* **2001**, *276*, 15616–15624.
- [52] L. O. Reid, A. H. Thomas, V. Herlax, M. L. Dantola, *Biochemistry* **2020**, *59*, 4213–4224.
- [53] E. Madrid, S. L. Horswell, *J. Electroanal. Chem.* **2018**, *819*, 338–346.
- [54] a) S. Reuter, T. von Woedtke, K. D. Weltmann, *J. Phys. D* **2018**, *51*; b) M. S. Mann, R. Tiede, K. Gavenis, G. Daeschlein, R. Bussiahn, K.-D. Weltmann, S. Emmert, T. v. Woedtke, R. Ahmed, *Clin. Plasma Med.* **2016**, *4*, 35–45.
- [55] M. Bern, Y. J. Kil, C. Becker, *Curr. Protoc. Bioinformatics* **2012**, *Chapter 13*, Unit13 20.
- [56] D. Van Der Spoel, E. Lindahl, B. Hess, G. Groenhof, A. E. Mark, H. J. Berendsen, *J. Comput. Chem.* **2005**, *26*, 1701–1718.
- [57] O. Trott, A. J. Olson, *J. Comput. Chem.* **2010**, *31*, 455–461.
- [58] S. Kim, J. Chen, T. Cheng, A. Gindulyte, J. He, S. He, Q. Li, B. A. Shoemaker, P. A. Thiessen, B. Yu, L. Zaslavsky, J. Zhang, E. E. Bolton, *Nucleic Acids Res.* **2019**, *47*, D1102–D1109.
- [59] D. S. Biovia, Vol. 936, Biovia, Dassault Systèmes, San Diego, CA, USA, **2017**.
- [60] M. D. Hanwell, D. E. Curtis, D. C. Lonie, T. Vandermeersch, E. Zurek, G. R. Hutchison, *J. Cheminf.* **2012**, *4*, 17.
- [61] W. L. DeLano, in *CCP4 Newsletter on protein crystallography*, Vol. 40, **2002**, pp. 82–92.

Manuscript received: June 26, 2021  
Accepted manuscript online: August 10, 2021  
Version of record online: September 15, 2021